WING-BODY YAWING MOMENT AND SIDEFORCE DERIVATIVES DUE TO SIDESLIP: N_v AND Y_v (WITH ADDENDUM A FOR NACELLE EFFECTS)

1. NOTATION AND UNITS (see Sketch 1.1)

The derivative notation used is that proposed in ARC R&M 3562 (Hopkin, 1970) and described in Item No. 86021. Coefficients and aeronormalised derivatives are evaluated in aerodynamic body axes with origin at the aircraft centre of gravity and with the wing span as the characteristic length. The derivatives N_v and Y_v are often written as $\partial C_n/\partial\beta$ and $\partial C_Y/\partial\beta$ or $C_{n\beta}$ and $C_{Y\beta}$ in other systems of notation, but attention must be paid to the reference dimensions used and it is to be noted that a constant datum value of V is employed in the Hopkin system.

		SI	British
A	wing aspect ratio, b^2/S		
b	wing span	m	ft
C_L	lift coefficient of equivalent wing, $L/½\rho V^2 S$		
C_n	yawing moment coefficient, $\mathcal{N}/½\rho V^2 Sb$		
C_Y	sideforce coefficient, $Y/½\rho V^2 S$		
d	maximum body width	m	ft
F	function allowing for effects on sideforce derivative of wing height and wing span to body width ratio (see Equation (2.3))		
F_W	factor for applying corrections for wing planform to function F		
h	maximum height of body section	m	ft
h_1, h_2	body section heights, at $0.25 l_b$ and $0.75 l_b$	m	ft
L	lift of equivalent wing	N	lbf
l	distance of yaw axis behind body nose	m	ft
l_b	overall body length	m	ft
$\mathcal{N}$	yawing moment	N m	lbf ft
N_v	aeronormalised yawing moment derivative due to sideslip (about general reference yaw axis), $N_v = (\partial\mathcal{N}/\partial v)/½\rho VSb$		
$N_{v\ mid}$	aeronormalised yawing moment derivative about yaw axis through mid-point of body length		
S	gross area of equivalent wing planform	m^2	ft^2
S_b	area of side elevation of body	m^2	ft^2

Issued June 1979
Reprinted with Amendments A and B, March 1999 – 23 pages
This page Amendment B

V	velocity of wing-body relative to air	m/s	ft/s
v	sideslip velocity	m/s	ft/s
Y	sideforce	N	lbf
Y_v	aeronormalised sideforce derivative due to sideslip, $Y_v = (\partial Y/\partial v)/\tfrac{1}{2}\rho VS$		
z	vertical position of quarter-chord point of wing root chord relative to body centre-line (positive for a low wing)	m	ft
α	angle of attack	radian	radian
β	sideslip angle, $\sin^{-1}(v/V)$	radian	radian
Γ	dihedral angle (assumed constant across wing semi-span), defined as angle between wing reference plane and projection of quarter-chord line on plane perpendicular to wing centre-line chord; the wing reference plane is that plane normal to plane of symmetry and containing wing centre-line chord	degree	degree
$\Lambda_{1/4}$	quarter-chord sweep of equivalent wing planform	degree	degree
λ	wing taper ratio (ratio of tip chord to centre-line chord)		
ρ	density of air	kg/m^3	slug/ft^3

Subscripts

wing	denotes isolated wing values

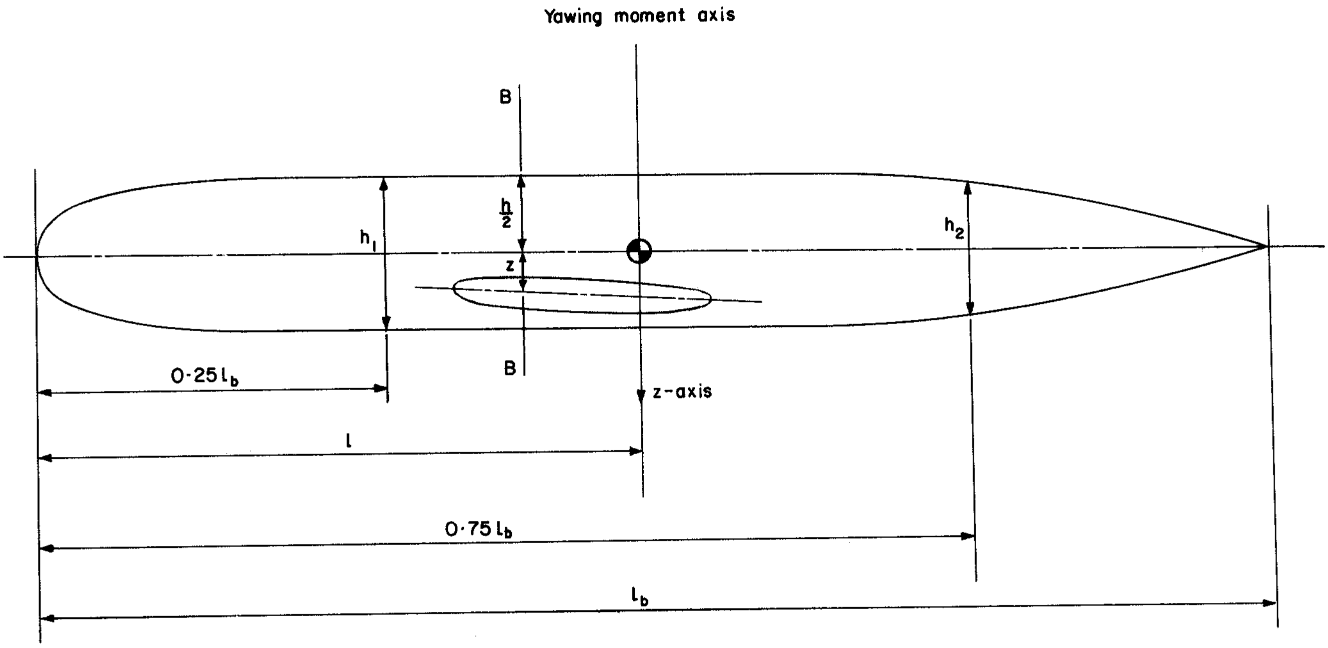

Sketch 1.1

This page Amendment B

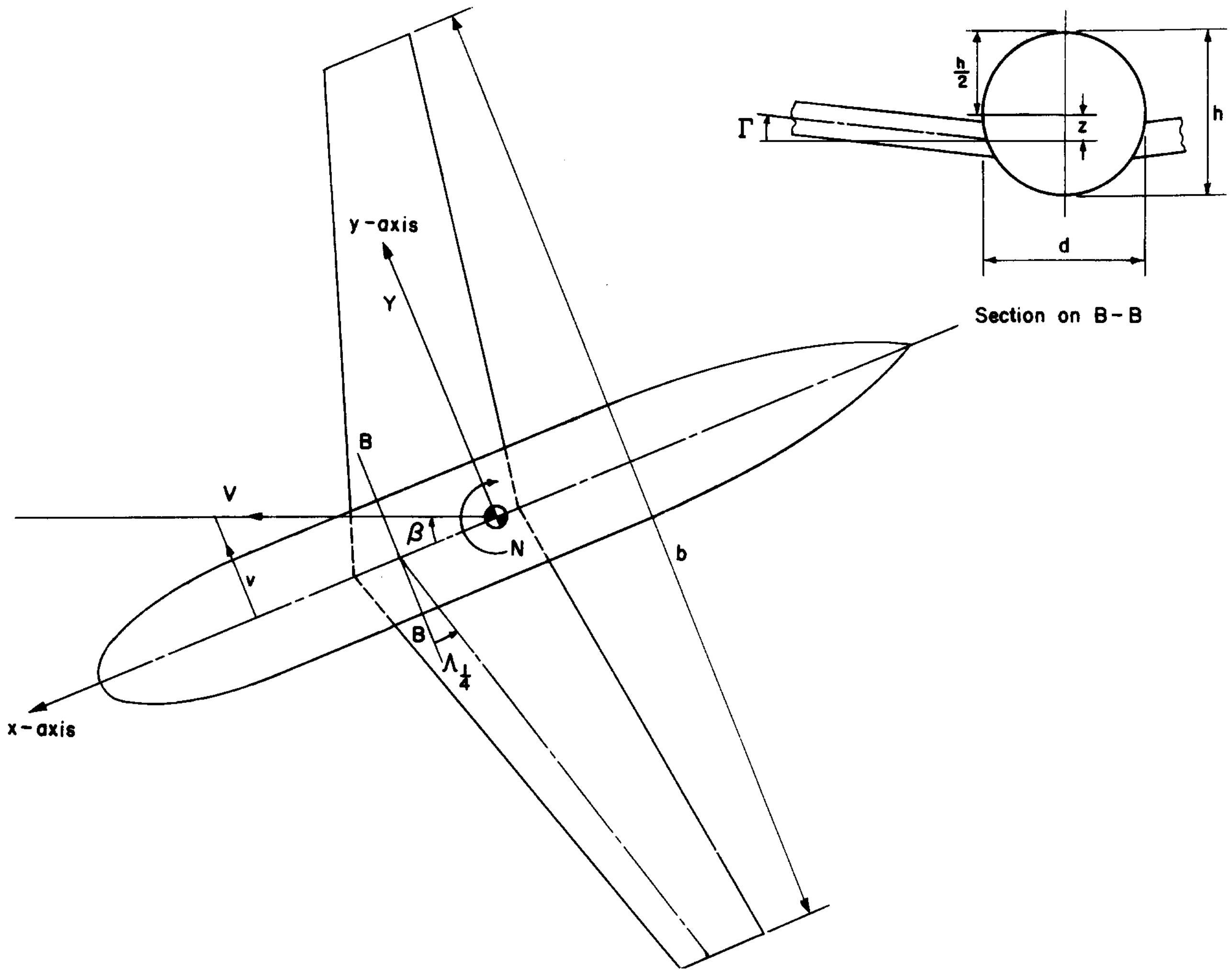

Sketch 1.1 (continued)

2. METHOD

2.1 Summary of Method

This Item provides a means of estimating the yawing moment and sideforce derivatives due to sideslip for wing-body combinations at small angles of attack and sideslip at subsonic speeds. For stability calculations an accurate prediction is more important for N_v than for Y_v and the data in this Item are primarily intended for predicting N_v. Because N_v is dependent on the choice of yaw axis position a knowledge of Y_v is needed to convert N_v from one axis position to another. An accurate estimate of Y_v is difficult and the method given may involve substantial errors for certain configurations (see Section 4.1) but it is considered adequate in allowing for changes in yaw axis position between $0.4l_b$ and $0.6l_b$ as, subject to that limitation, quite large uncertainties in Y_v do not give rise to significant errors in N_v.

The yawing moment derivative about a yaw axis through the mid-point of the body is given by the empirical relation

$$-N_{v\,mid} = \left[0.2575 + \frac{l_b^2}{S_b}\left\{0.0008\frac{l_b^2}{S_b} - 0.024\right\}\right]\left[1.39\left(\frac{h_1}{h_2}\right)^{½} - 0.39\right]\left[\frac{S_b l_b}{Sb}\right], \tag{2.1}$$

and is independent of wing geometry (but see Section 2.3 for discussion on effect of sweepback). Figure 1 presents the parameter $-N_{v\,mid}\,[Sb/S_b l_b]$ plotted against l_b^2/S_b and h_1/h_2. For an axis at a distance l behind the body nose the yawing moment derivative is given by

$$N_v = N_{v\,mid} + \frac{(l - 0.5l_b)}{b}Y_v, \tag{2.2}$$

where the sideforce derivative is given by the empirical relation

$$-Y_v = \left[0.0714 + 0.674\frac{h^2}{S_b} + \frac{hbFF_W}{S_b}\left(4.95\frac{|z|}{h} - 0.12\right)\right]\frac{S_b}{S} + 0.006|\,\Gamma\,|. \tag{2.3}$$

Figure 2 presents the function F as a carpet in terms of $|z|/h$ and b/d. Figure 3 presents the factor F_W as a carpet in terms of A and λ. (See Section 2.3 for discussion on effect of sweepback.)

2.2 Basis of Method

Equation (2.1) was developed by analysing the wind-tunnel data in Derivations 2 to 41 and deducing an empirical correlation for $N_{v\,mid}\,[Sb/S_b l_b]$ in terms of the parameters l_b^2/S_b and h_1/h_2. The bracketed expression involving l_b^2/S_b allows for the gross shape of the body, and the second bracketed expression involving h_1/h_2 allows approximately for differences between the forebody and afterbody shapes. The experimental data studied showed that wing dihedral angle had no significant effect on $N_{v\,mid}$.

Equation (2.3) was developed by first analysing the wind-tunnel data in Derivations 2 to 41 for configurations with mid-wings (z = 0) without dihedral. This led to the first and second terms in Equation (2.3). Two further terms were then added to allow for the effects of wing height and wing dihedral angle. The method of allowing for wing height is based on the one suggested in Derivation 34 which uses the theoretical change in the flow circulation around the wing caused by the wing-body sideslipping. The maximum change in circulation occurs close to the wing-root chord and is taken as a measure of the change in pressure produced in the region of the wing-body junction. The pressure changes on the two sides of the body are of opposite sign and result in a sideforce. For use in Equation (2.3) of this Item two functions, F and F_W, based on the maximum change in dimensionless circulation have been calculated by applying lifting-line theory to a series of wings of trapezoidal planform and the results are given in Figures 2 and 3. (Wings with planforms other than trapezoidal should be replaced by equivalent trapezoidal planforms as described in Item No. 76015, Reference 44.) The function F allows for the effects of wing height and wing span to body width ratio; F_W is a factor applied to F to allow for wing aspect ratio and taper ratio effects. The variation of sideforce derivative with $|z|/h$ was obtained by choosing the best linear fit to the experimental data. (It should be noted that F is zero when z is zero and so the term –0.12 in Equation (2.3) does not give rise to a sideforce for bodies with mid-wings.) The term in Equation (2.3) that allows for wing dihedral was taken from Derivation 1 which contains data from wind-tunnel tests on isolated wings of aspect ratio 6 at varying angles of dihedral and with sweep angles between –4° and 14°.

2.3 Effect of Wing Sweepback and Lift Coefficient

The equations given in Section 2.1 for predicting N_v and Y_v were developed from experimental data obtained at low angles of attack and do not include any effects due to wing sweepback. This is because at low lift coefficients the values of N_v and Y_v for isolated wings without dihedral are small. For example, with a yaw axis through the wing aerodynamic centre, the theoretical equations developed in References 42 and 43 for predicting the stability derivatives of isolated wings give $N_{v\ wing} < 0.004$ and $Y_{v\ wing} < 0.003$ for $C_L = 0.3$ and $\Lambda_{1/4} \le 25°$. At higher angles of sweepback the wing contribution becomes larger and for $C_L = 0.3$, $\Lambda_{1/4} = 50°$, $N_{v\ wing} \approx 0.008$ and $Y_{v\ wing} \approx 0.017$. (Note that the wing-alone values are of opposite sign to the wing-body values.) The isolated wing values vary as C_L^2 and are therefore more significant at higher lift coefficients ($C_L \approx 0.5$, say) particularly for moderate to high sweepback angles. In general, provided the flow over the wing is not separated, the experimental data show that for wing-body combinations N_v and Y_v decrease in magnitude as C_L increases. However, this decrease is often less than that suggested by the equations in References 42 and 43, possibly because of wing-body interference effects. As this Item is primarily concerned with low angles of attack and sideslip a generalised method for predicting high C_L effects has not been attempted. Estimates of the variation of N_v and Y_v with C_L made by adding wing-alone values to the values predicted by Equations (2.2) and (2.3) should be treated cautiously.

3. EFFECT OF JET ENGINE NACELLES

It is important to note that the method described in Section 2 applies to wing-body configurations only. Wind-tunnel data in Derivations 38 to 40 show that the presence of jet-engine nacelles mounted on under-wing pylons can significantly change the lateral stability derivatives from their wing-body values, and in this situation Equations (2.2) and (2.3) do not provide adequate estimates of N_v and Y_v. Jet-engine nacelles mounted on the rear of the body, however, have little effect on N_v and Y_v when fin and tailplane are not present, and Equations (2.2) and (2.3) may be used. When the fin and tailplane are present then the addition of nacelles to the rear fuselage can cause large changes in N_v and Y_v due to interference between the nacelles and tail surfaces. Thus, in this case, a simple combination of estimated fin and tailplane contributions to N_v and Y_v with the wing-body values from Equations (2.2) and (2.3) may give derivatives which are substantially different from those measured experimentally for the complete aircraft with nacelles fitted.

Addendum A of this Item gives an assessment of the size of the nacelle contribution to N_v and Y_v, based on the available experimental data.

4. ACCURACY AND APPLICABILITY

4.1 Accuracy

For wing-body configurations 80 per cent of the data for N_v in Derivations 2 to 41 are predicted to within ± 0.01 and 90 per cent to within ± 0.02; 90 per cent of the data for Y_v are predicted to within ± 0.05. However, it should be noted that for two configurations the method overestimates Y_v by 50 per cent or more. These two configurations are the only ones having wings (with anhedral) mounted at the top of the fuselage ($z/h \approx -0.5$); the values of Y_v for configurations with wings mounted less high on the fuselage ($0 > z/h > -0.4$) are not overestimated and this apparent discrepancy has not yet been explained. Data for low wing configurations with $z/h \approx 0.5$ are predicted satisfactorily.

For wing-body-nacelle configurations, using the correction terms suggested in Section 3 for under-wing nacelles, the data in Derivations 36 and 38 to 40 are generally predicted to within ± 0.02 for N_v and to within ± 0.1 for Y_v.

4.2 Applicability

The data in this Item are for wing-body combinations at small angles of attack and sideslip, in the region where the rates of change of sideforce and yawing moment with sideslip are essentially linear and independent of the angle of attack. Typically, these conditions are satisfied for angles of attack less than about 6° to 8° and angles of sideslip less than 10°. Most of the experimental data studied were for low subsonic Mach numbers, but a few data were available for Mach numbers up to 0.8 and these showed no significant departures from the low-speed results. The method assumes that the flow over the configuration is fully attached and wholly subsonic and that any wing slats and flaps are not deployed.

Table 4.1 shows the ranges of wing-body geometric parameters studied in the preparation of this Item and the method should be used with caution for configurations with geometries that are outside these ranges. In particular, the limitations on l/l_b should be noted because Y_v is, in general, less well predicted than N_v and, as shown by Equation (2.2), uncertainties in Y_v give rise to uncertainties in N_v which increase as the distance of the yawing moment axis from the body mid-point increases. Most of the data considered were in the range $0.4 \le l/l_b \le 0.6$, with a few data at $l/l_b \approx 0.3$. The magnitudes of the changes in N_v caused by axis position changes were typically between 0.01 and 0.02.

TABLE 4.1 Range of Geometries Considered

Parameter	*Range*
A	2 to 9
b/h	4 to 11
l_b/h	5 to 13
l/l_b	(0.3) 0.4 to 0.6
z/h	–0.5 to 0.5
Γ	–10° to +10°
λ	0 to 1
$\Lambda_{1/4}$	0 to 60°

The data apply directly to wing-body configurations with axisymmetric bodies. The accuracy of the method is not, however, affected for bodies with rear-fuselage upsweeps typical of current jet transport aircraft. Derivation 4 contains some data for a body of elliptical cross section, and Derivations 24 and 30 contain a limited number of data on configurations with bodies of square and rectangular cross sections, with slightly rounded corners. To investigate the effects of cross-sectional shape the side elevations of the non-circular bodies were used to provide the geometric parameters needed in the method, with the parameter $2b/(h + d)$ being used instead of b/d for determining the function F.

Table 4.2 summarises the results of comparing the experimental effects of body cross-section on $N_{v\,mid}$ and Y_v with those predicted by the above method. This table was generated from a small number of data and therefore the values quoted are intended only as an indication of the changes that can occur when the body cross-section is significantly non-circular.

TABLE 4.2 Percentage Increases in $N_{v\ mid}$ and Y_v for Bodies of Non-Circular Cross-Section

Cross-Section	Height/ Width	Percentage increase in $N_{v\ mid}$			Percentage increase in Y_v		
		High Wing $\left(\frac{z}{h} \approx -0.4\right)$	Mid Wing $\left(\frac{z}{h} = 0\right)$	Low Wing $\left(\frac{z}{h} \approx 0.4\right)$	High Wing $\left(\frac{z}{h} \approx -0.4\right)$	Mid Wing $\left(\frac{z}{h} = 0\right)$	Low Wing $\left(\frac{z}{h} \approx 0.4\right)$
Ellipse[*] 0	1.75	20	40	20	0	10	0
Upright Rectangle ▯	1.7	–	20	–	–	30	–
Square □	1	30	30	30	20	20	20
Transverse Rectangle ▭	0.6	–	10	–	–	60	–

[*] The N_v data for the elliptical bodies were subject to greater uncertainty than normal as the yaw axis was well forward at $l/l_b = 0.32$ and so uncertainties in Y_v could be responsible to some extent for the large increases in $N_{v\ mid}$.

5. DERIVATION AND REFERENCES

5.1 Derivation

The Derivation lists selected sources that have assisted in the preparation of this Item.

1.	BAMBER, M.J. HOUSE, R.O.	Wind-tunnel investigation of effect of yaw on lateral-stability characteristics. I – Four NACA 23012 wings of various planforms with and without dihedral. NACA tech. Note 703, 1939.
2.	BAMBER, M.J. HOUSE, R.O.	Wind-tunnel investigation of effect of yaw on lateral-stability characteristics. II – Rectangular NACA 23012 wing with a circular fuselage and a fin. NACA tech. Note 730, 1939.
3.	RECANT, I.G. WALLACE, A.R.	Wind-tunnel investigation of effect of yaw on lateral-stability characteristics. III – Symmetrically tapered wing at various positions on circular fuselage with and without a vertical tail. NACA tech. Note 825, 1941.
4.	HOUSE, R.O. WALLACE, A.R.	Wind-tunnel investigation of effect of interference on lateral-stability characteristics of four NACA 23012 wings, an elliptical and a circular fuselage and vertical fins. NACA Rep. 705, 1941.
5.	WALLACE, A.R. TURNER, T.R.	Wind-tunnel investigation of effect of yaw on lateral-stability characteristics. V – Symmetrically tapered wing with a circular fuselage having a horizontal and vertical tail. NACA ARR 3F23 (TIL 456), 1943.
6.	SALMI, R.J. CONNER, D.W. GRAHAM, R.R.	Effects of fuselage on the aerodynamic characteristics of a 42° sweptback wing at Reynolds numbers to 8,000,000. NACA RM L7E13 (TIL 1185), 1947.

7. BIRD, D.J. LICHTENSTEIN, J.H. — Investigation of the influence of fuselage and tail surfaces on low-speed static stability and rolling characteristics of a swept-wing model. NACA tech. Note 2741, 1947.

8. SALMI, R.J. — Yaw characteristics of a 52° sweptback wing of NACA 64-112 section with a fuselage and with leading edge and split flaps at Reynolds numbers from 1.93×10^6 to 6.00×10^6. NACA RM L8H12 (TIL 1984), 1948.

9. JAQUET, B.M. BREWER, J.D. — Effects of various outboard and central fins on low-speed static stability and rolling characteristics of a triangular-wing model. NACA RM L9E18 (TIL 2137), 1949.

10. LETKO, W. WOLHART, W.D. — Effect of sweepback on the low-speed static and rolling stability derivatives of thin tapered wings of aspect ratio 4. NACA RM L9F14 (TIL 2288), 1949.

11. BREWER, J.D. LICHTENSTEIN, J.H. — Effect of horizontal tail on low-speed static lateral-stability characteristics of a model having 45° sweptback wing and tail surfaces. NACA tech. Note 2010, 1949.

12. LETKO, W. RILEY, R.R. — Effects of an unswept wing on the contribution of unswept-tail configurations to low-speed static- and rolling-stability derivatives of a midwing airplane model. NACA tech. Note 2175, 1950.

13. GOODMAN, A. — Effects of wing position and horizontal-tail position on the static stability characteristics of models with unswept and 45° sweptback surfaces with some reference to mutual interference. NACA tech. Note 2504, 1951.

14. QUEIJO, M.J. WOLHART, W.D. — Experimental investigation of the effect of vertical-tail size and length and of fuselage shape and length on the static lateral-stability characteristics of a model with 45° swept-back wing and tail surfaces. NACA Rep. 1049, 1951.

15. KUHN, R.E. FOURNIER, P.G. — Wind-tunnel investigation of the static lateral-stability characteristics of wing-fuselage combinations at high subsonic speeds. Sweep series. NACA RM L52G11a (TIL 3330), 1952.

16. GRAHAM, D. KOENIG, D.G. — Tests in the Ames 40- by 80-foot wind-tunnel of an airplane configuration with an aspect ratio 2 triangular wing and an all-movable horizontal tail – lateral characteristics. NACA RM A51L03 (TIL 4280), 1952.

17. KUHN, R.E. DRAPER, J.W. — Wind-tunnel investigation of the effects of geometric dihedral on the aerodynamic characteristics in pitch and sideslip of an unswept- and a 45° sweptback-wing-fuselage combination at high subsonic speeds. NACA RM L53F09 (TIL 3829), 1953.

18. WIGGINS, J.W. FOURNIER, P.G. — Wind-tunnel investigation of the static lateral-stability characteristics of wing-fuselage combinations at high subsonic speeds. Taper ratio series. NACA tech. Note 4174, 1953.

19. WIGGINS, J.W.
KUHN, R.E.
FOURNIER, P.G.
Wind-tunnel investigation to determine the horizontal- and vertical-tail contributions to the static lateral-stability characteristics of a complete-model swept-wing configuration at high subsonic speeds. NACA tech. Note 3818, 1953.

20. FOURNIER, P.G.
BYRNES, A.L.
Wind-tunnel investigation of the static lateral-stability characteristics of wing-fuselage combinations at high subsonic speeds. Aspect ratio series. NACA RM L52L18 (TIL 3624), 1953.

21. GRINER, R.F.
Static lateral-stability characteristics of an airplane model having a 47.7° sweptback wing of aspect ratio 6 and the contribution of various model components at a Reynolds number of 4.45×10^6. NACA RM L53G09 (TIL 3885), 1953.

22. CHRISTENSEN, F.B.
An experimental investigation of four triangular-wing-body combinations in sideslip at Mach Nos 0.6, 0.9, 1.4 and 1.7. NACA RM A53L22 (TIL 4119), 1954.

23. GOODSON, K.W.
BECHT, R.E.
Wind-tunnel investigation at high subsonic speeds of the stability characteristics of a complete model having sweptback-, M-, W-, and cranked-wing planforms and several horizontal-tail locations. NACA RM L54C29 (TIL 4231), 1954.

24. LETKO, W.
WILLIAMS, J.L.
Experimental investigation at low speed of effects of fuselage cross-section on static longitudinal and lateral-stability characteristics of models having 0° and 45° sweptback surfaces. NACA tech. Note 3551, 1955.

25. JAQUET, B.M.
WILLIAMS, J.L.
Wind-tunnel investigation at low speed of effect of size and position of closed air ducts on static longitudinal and static lateral-stability characteristics of unswept-midwing models having wings of aspect ratio 2, 4 and 6. NACA tech. Note 3481, 1955.

26. WOLHART, W.D.
THOMAS, D.F.
Static longitudinal and lateral-stability characteristics at low speed of unswept-midwing models having wings with an aspect ratio of 2, 4 or 6. NACA tech. Note 3649, 1955.

27. SAVAGE, H.F.
TINLING, B.E.
The subsonic static aerodynamic characteristics of an airplane model having a triangular wing of aspect ratio 3. II – Lateral and directional characteristics. NACA tech. Note 4042, 1955.

28. GOODMAN, A.
THOMAS, D.F.
Effects of wing position and fuselage size on the low-speed static and rolling-stability characteristics of a delta-wing model. NACA Rep. 1224, 1955.

29. FOURNIER, P.G.
Low-speed static stability characteristics of a complete model with an M-wing in mid and high positions and with three horizontal-tail heights. NACA RM L55J06 (TIL 4944), 1956.

30. KING, T.J.
Wind-tunnel investigation at high subsonic speeds of some effects of fuselage cross-section shape and wing height on the static longitudinal and lateral-stability characteristics of a model having a 45° swept wing. NACA RM L55J25 (TIL 4960), 1956.

31. SLEEMAN, W.C. — An experimental study at high subsonic speeds of several tail configurations on a model having a 45° sweptback wing. NACA RM L57C08 (TIL 5495), 1957.

32. LICHTENSTEIN, J.H.
WILLIAMS, J.L. — Effect of frequency of sideslipping motion on the lateral-stability derivatives of a typical delta-wing airplane. NACA RM L57F07 (TIL 5664), 1957.

33. THOMAS, D.F.
WOLHART, W.D. — Static longitudinal and lateral-stability characteristics at low speed of 45° sweptback-midwing models having wings with an aspect ratio of 2, 4 or 6. NACA tech. Note 4077, 1957.

34. GERSTEN, K.
HUMMEL, D. — Experimentelle und theoretische Untersuchungen über die Interferenzeinflüsse an schiebenden Flugel-Rumf-Anordnungen mit Pfeil-und Deltaflugeln. DLR FB 66-77, 1966.

35. EYRE, R.C.W.
BUTLER, S.F.J. — Low-speed wind-tunnel tests on an AR 8 swept wing subsonic transport research model with BLC blowing over nose and rear flaps for high-lift. RAE tech. Rep. 67112, 1967.

36. RAY, E.J. — Effect of large sideslip angles on stability characteristics of a T-tail transport configuration. NACA tech. Memor. TM X-1665, 1968.

37. HENDERSON, W.P.
HUFFMAN, J.K. — Lateral-directional stability characteristics of a wing-fuselage configuration at angles of attack up to 44°. NASA tech. Memor. TM X-3087, 1974.

38. – — Unpublished wind-tunnel data from Aérospatiale, Toulouse, France.

39. – — Unpublished wind-tunnel data from Aircraft Research Association.

40. – — Unpublished wind-tunnel data from British Aerospace, Aircraft Group, Weybridge-Bristol, Hatfield-Chester and Manchester Divisions.

41. – — Unpublished wind-tunnel data from Saab-Scania, Sweden.

5.2 References

The References given are recommended sources of information supplementary to that in this Item.

42. TOLL, T.A.
QUEIJO, M.J. — Approximate relations and charts for low-speed stability derivatives of swept wings. NACA tech. Note 1581, 1948.

43. FISHER, L.R. — Approximate corrections for the effects of compressibility on the subsonic stability derivatives of swept wings. NACA tech. Note 1854, 1949.

44. – — Aerodynamic centre of wing-fuselage combinations. Engineering Sciences Data Item No. 76015, 1976.

6. EXAMPLE

Find the subsonic yawing moment derivative due to sideslip of the low-wing-body combination shown in Sketch 6.1 for an axis positioned 19.4 m from the body nose. Small angles of attack and sideslip may be assumed. The wing planform is the same as that used in the Example to Item No. 76015, in which the properties of the equivalent trapezoidal wing planform are calculated to be $A = 6.845$, $S = 149.6\ \text{m}^2$ and $\lambda = 0.472$. The area of the side elevation of the body is $122\ \text{m}^2$, the wing has a dihedral angle of 2.5° and the cross section of the body is circular.

The yawing moment derivative N_v about a yaw axis through the mid-point of the body is given by Equation (2.1),

$$-N_{v\,mid} = \left[0.2575 + \frac{l_b^2}{S_b}\left\{0.0008\frac{l_b^2}{S_b} - 0.024\right\}\right]\left[1.39\left(\frac{h_1}{h_2}\right)^{½} - 0.39\right]\left[\frac{S_b l_b}{Sb}\right]$$

$$= \left[0.2575 + \frac{36^2}{122}\left\{0.0008 \times \frac{36^2}{122} - 0.024\right\}\right]\left[1.39\left(\frac{4}{4}\right)^{½} - 0.39\right]\left[\frac{S_b l_b}{Sb}\right]$$

$$= 0.093 \times 1 \times \left[\frac{S_b l_b}{Sb}\right]$$

$$= 0.093\left[\frac{S_b l_b}{Sb}\right].$$

(Alternatively Figure 1 may be used with $l_b^2/S_b = 36^2/122 = 10.62$ and $h_1/h_2 = 1$ to obtain $-N_{v\,mid} = 0.093(S_b l_b/Sb)$.)

Therefore,

$$-N_{v\,mid} = 0.093\left[\frac{122 \times 36}{149.6 \times 32}\right]$$

$$= 0.085.$$

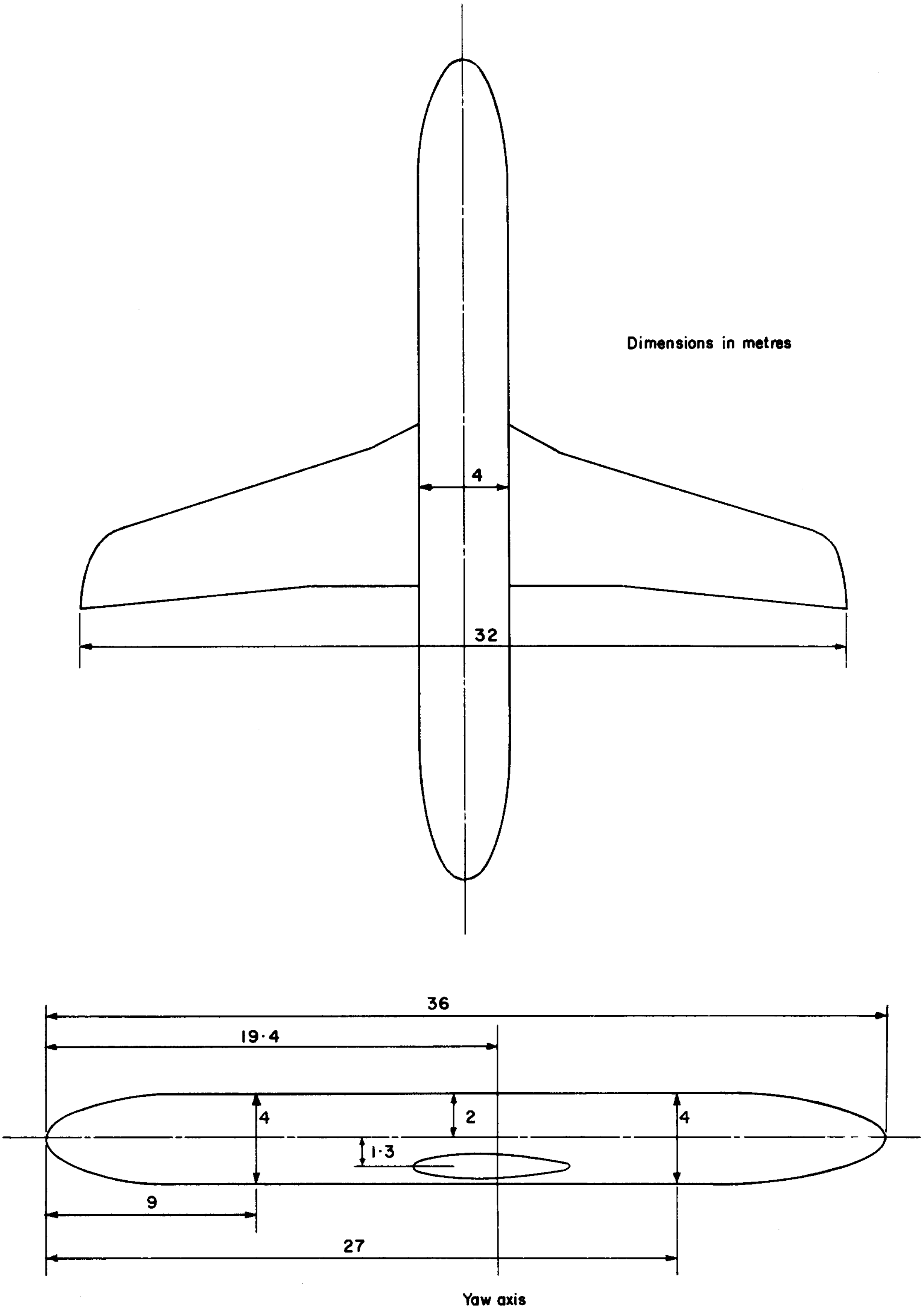

Sketch 6.1

The sideforce derivative is given by Equation (2.3),

$$-Y_v = \left[0.0714 + 0.674\frac{h^2}{S_b} + \frac{hbFF_W}{S_b}\left(4.95\frac{|z|}{h} - 0.12\right)\right]\frac{S_b}{S} + 0.006|\,\Gamma\,|\,.$$

From Figure 2 with $|z|/h = 1.3/4 = 0.325$ and $b/d = 32/4 = 8$, $F = 0.053$.

From Figure 3 with $A = 6.845$ and $\lambda = 0.472$, $F_W = 0.970$.

Therefore

$$-Y_v = \left[0.0714 + 0.674 \times \frac{4^2}{122} + \frac{4 \times 32 \times 0.053 \times 0.970}{122} \times \left(4.95 \times \frac{|1.3|}{4} - 0.12\right)\right]\frac{122}{149.6} + 0.006|\,2.5\,|$$

$= (0.0714 + 0.0884 + 0.0803) \times 0.816 + 0.015$

$= 0.196 + 0.015$

$= 0.211.$

The yawing moment about the specified yaw axis is calculated from Equation (2.2),

$$N_v = N_{v\,mid} + \frac{(l - 0.5l_b)}{b}Y_v$$

$$= -0.085 + \frac{(19.4 - 0.5 \times 36)(-0.211)}{32}$$

$= -0.085 - 0.009$

$= -0.094.$

Thus for the configuration in Sketch 6.1 the required yawing moment derivative is $N_v = -0.094$.

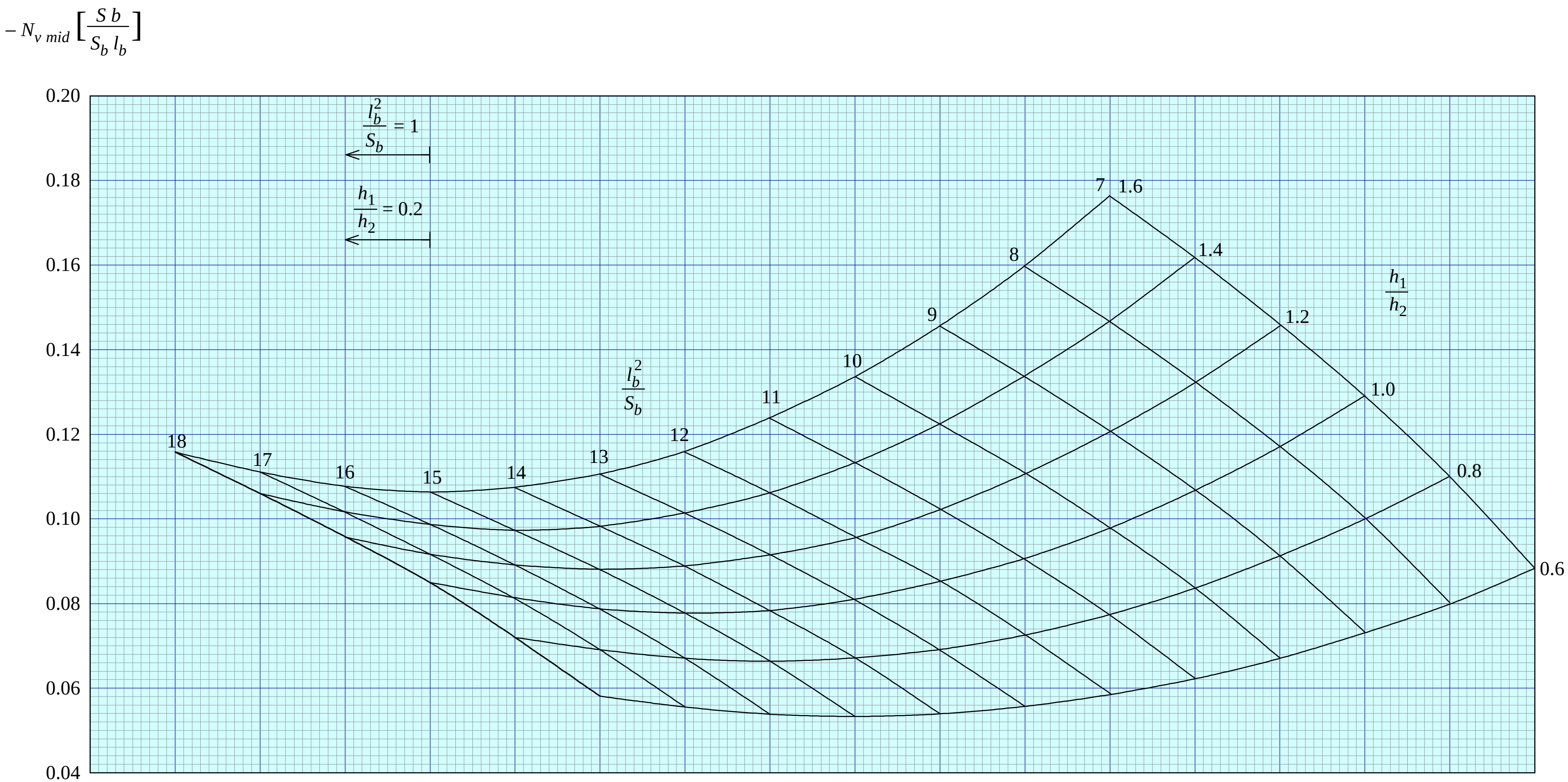

FIGURE 1 YAWING MOMENT DERIVATIVE

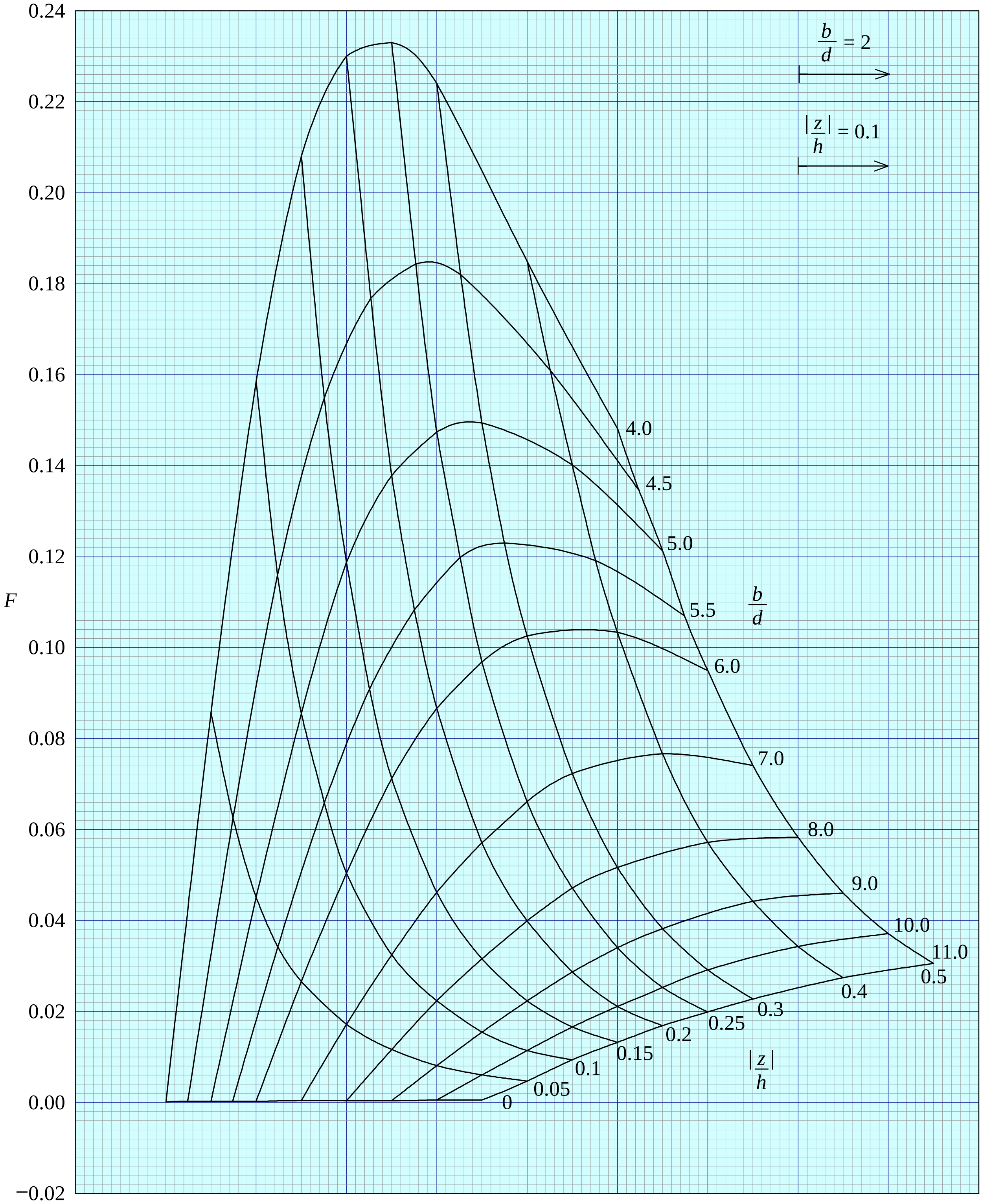

FIGURE 2 EFFECT OF WING HEIGHT AND BODY WIDTH FUNCTION

This page Amendment B

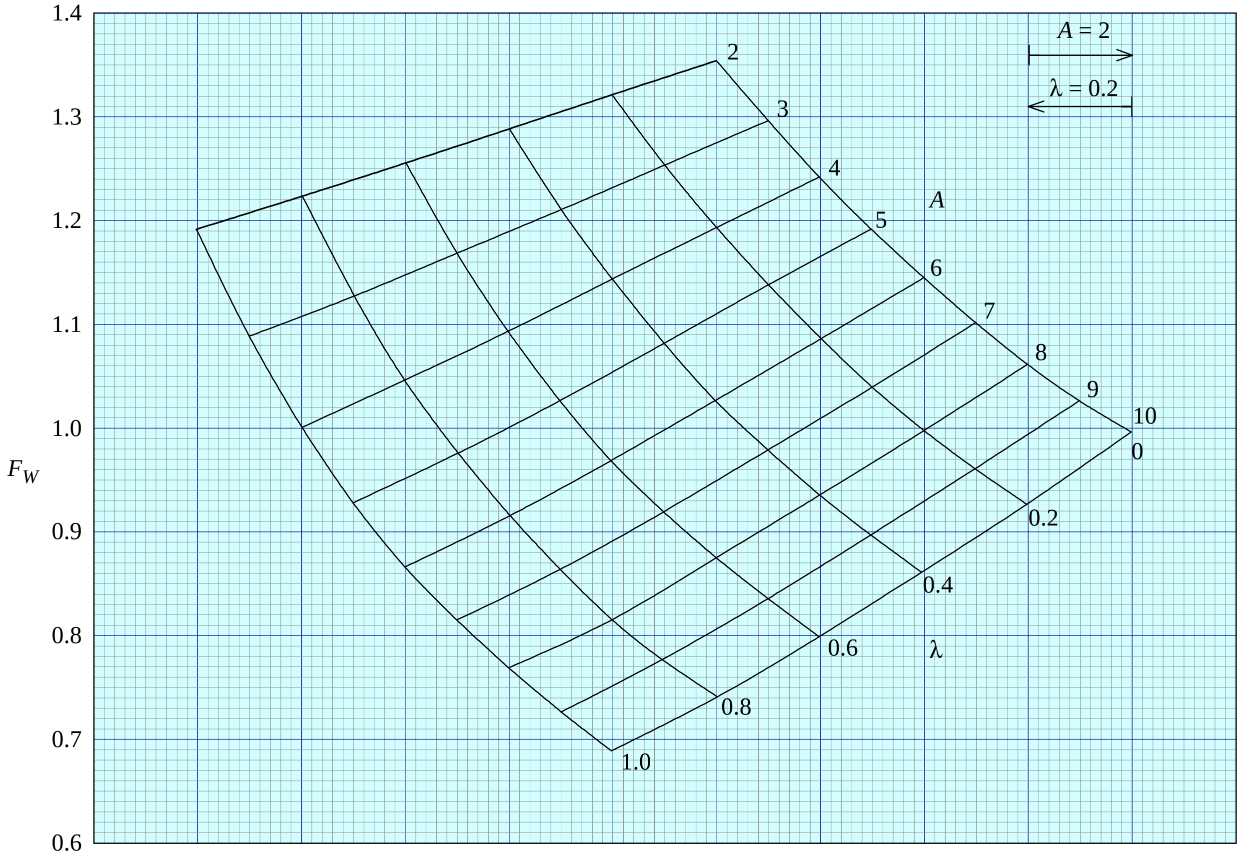

FIGURE 3 WING PLANFORM FACTOR

ADDENDUM A EFFECT OF JET-ENGINE NACELLES

A1. ADDITIONAL NOTATION AND UNITS (see Sketch A1.1)

		SI	*British*
l_n	overall length of nacelle	m	ft
m_0	distance of nacelle leading-edge forward of moment reference point	m	ft
$(N_v)_n$	contribution to N_v from pair of nacelles, one on each half wing		
s	wing semi-span	m	ft
s_n	spanwise distance from body centre-line to nacelle centre-line	m	ft
$w_{n\ e}$	nacelle exit diameter	m	ft
$w_{n\ max}$	maximum depth of nacelle	m	ft
$(Y_v)_n$	contribution to Y_v from pair of nacelles, one on each half wing		
z_n	distance of nacelle centre-line below wing-pylon junction	m	ft

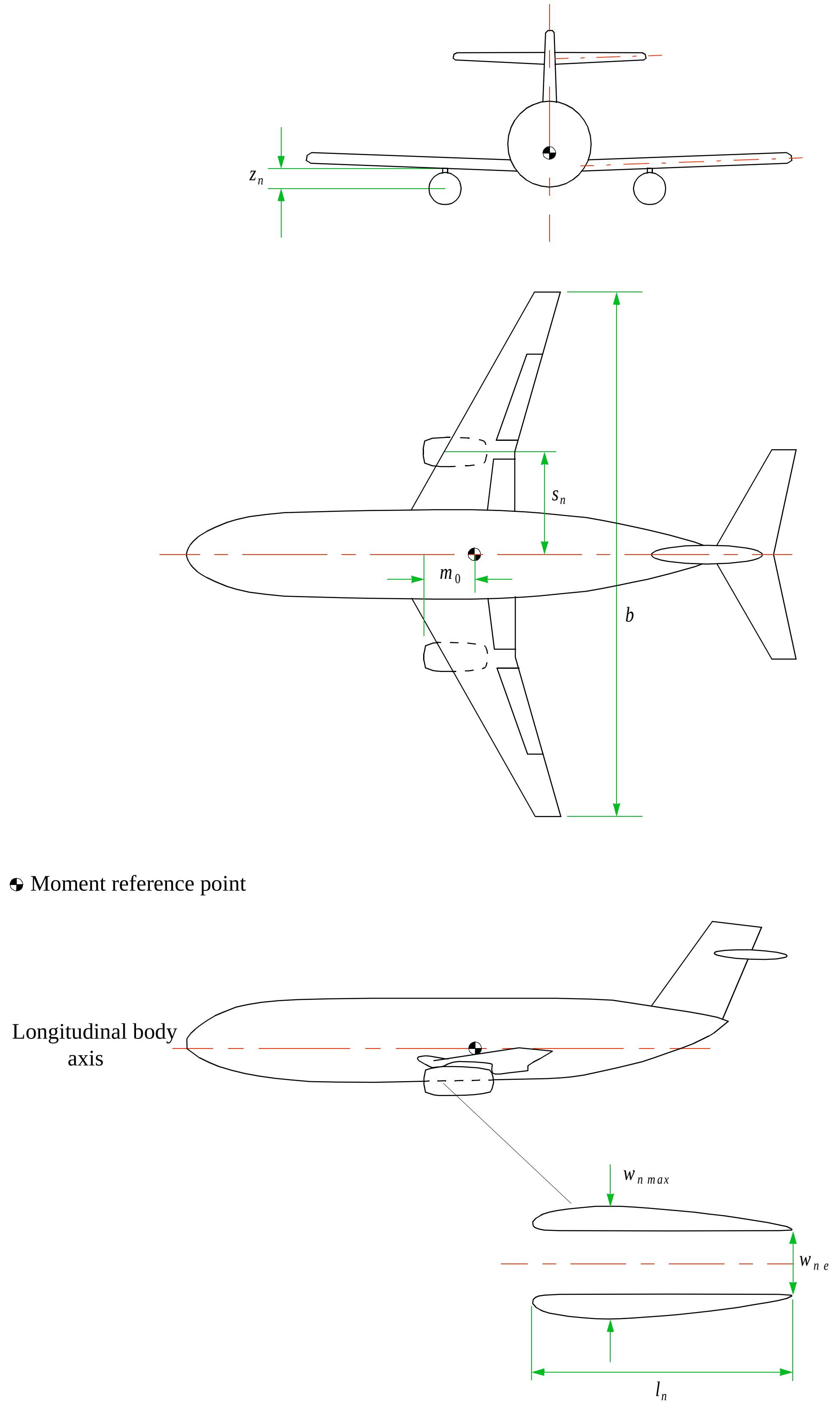

z_n
s_n
m_0
b
Moment reference point
Longitudinal body axis
$w_{n\,max}$
$w_{n\,e}$
l_n

Sketch A1.1

A2. INTRODUCTION

A limited number of wind tunnel data are available for aircraft models, typical of civil jet transports, which have been tested both with and without free-flow nacelles of the type customarily fitted in wind-tunnel tests to simulate the presence of jet-engine nacelles. This enables some guidance to be given on the effect of jet-engine nacelles on Y_v and N_v, but it is emphasised that the range of experimental data is limited and any estimates of nacelle effects must be used with caution.

A3. REAR-BODY MOUNTED NACELLES

An examination of wind-tunnel data from Derivation 40 for three low-wing aircraft with wing aspect ratios in the range 7 to 7.5 indicates that nacelles mounted on the rear part of the body have little effect on Y_v and N_v, when there is no fin or tailplane present. When the fin and tailplane are present then addition of the nacelles can give rise to significant changes in Y_v and N_v due to interference between the nacelles and the tail surfaces. In one particular case, it has been recorded that for nacelles mounted close to a fin, there was an increase in $-Y_v$ of 0.10 and, for a moment reference point close to the wing aerodynamic centre, an increase in N_v of 0.024. Care is therefore needed when values of Y_v and N_v for a complete aircraft are estimated by combining the predicted contributions of the tail surfaces with the predicted wing-body values.

A4. UNDER-WING MOUNTED NACELLES

Wind-tunnel data for nacelles mounted on under-wing pylons are available from Derivations 39, 40 and A1 for a small number of tests on both high-wing and low-wing multi-engine aircraft with wings of aspect ratios in the range 7.5 to 10.

For a pair of nacelles, one mounted on each half-wing, the best correlation of the available data has been found to be

$$(Y_v)_n = -\pi w_{n\ max}^2 \left(\frac{z_n + 0.5 w_{n\ max}}{w_{n\ max}}\right)^{1.5} \Big/ S \tag{A4.1}$$

and

$$(N_v)_n = -\left[\pi w_{n\ max}^2 (m_0 - w_{n\ max}) + \pi w_{n\ e}^2 l_n\right] \Big/ Sb \,. \tag{A4.2}$$

In Equation (A4.1) the external flow around each nacelle is assumed to generate a basic sideforce derivative $-(\pi/2) w_{n\ max}^2/S$, which is increased by the factor $[(z_n + 0.5 w_{n\ max})/w_{n\ max}]^{1.5}$ to allow empirically for the presence of the pylon.

In the calculation of the yawing moment derivative the point of action of the basic external-flow sideforce derivative is assumed to be a distance $w_{n\ max}$ aft of the nacelle lip. It is further assumed that the internal flow through each nacelle contributes a couple $-(\pi/2) w_{n\ e}^2 l_n/Sb$. It was found to be unnecessary to make any explicit allowance for the pylon.

For a four-engine configuration the estimates of Equations (A4.1) and (A4.2) would need to be evaluated for the inboard and outboard pairs separately and the results summed.

Sketches A4.1 and A4.2 compare predicted and experimental values of $\Sigma(Y_v)_n$ and $\Sigma(N_v)_n$ (for a moment reference point close to the wing aerodynamic centre), where Σ denotes a summation of two pairs for four-nacelle configurations.

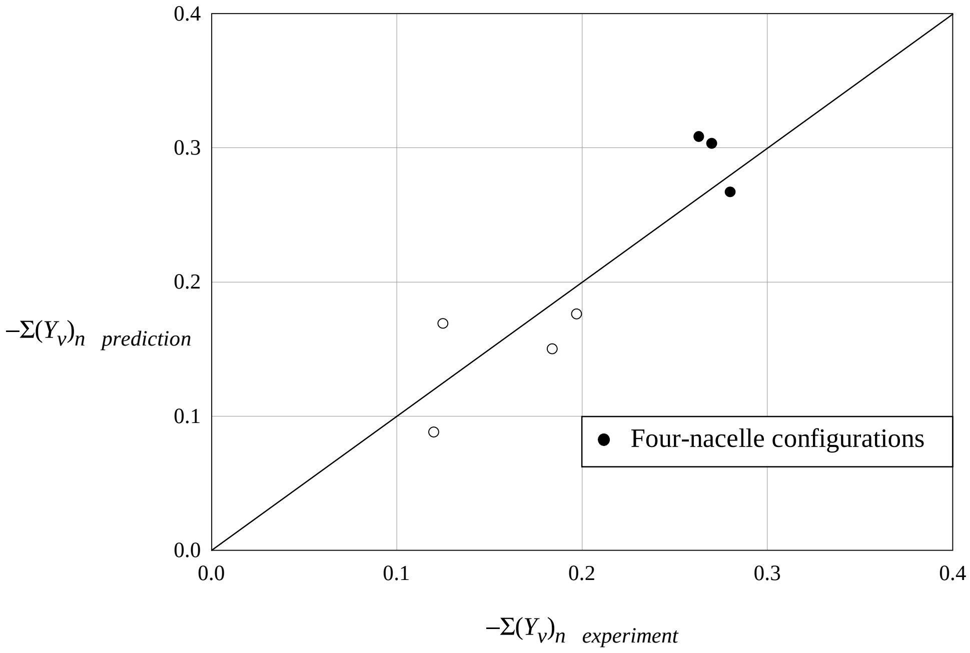

Sketch A4.1

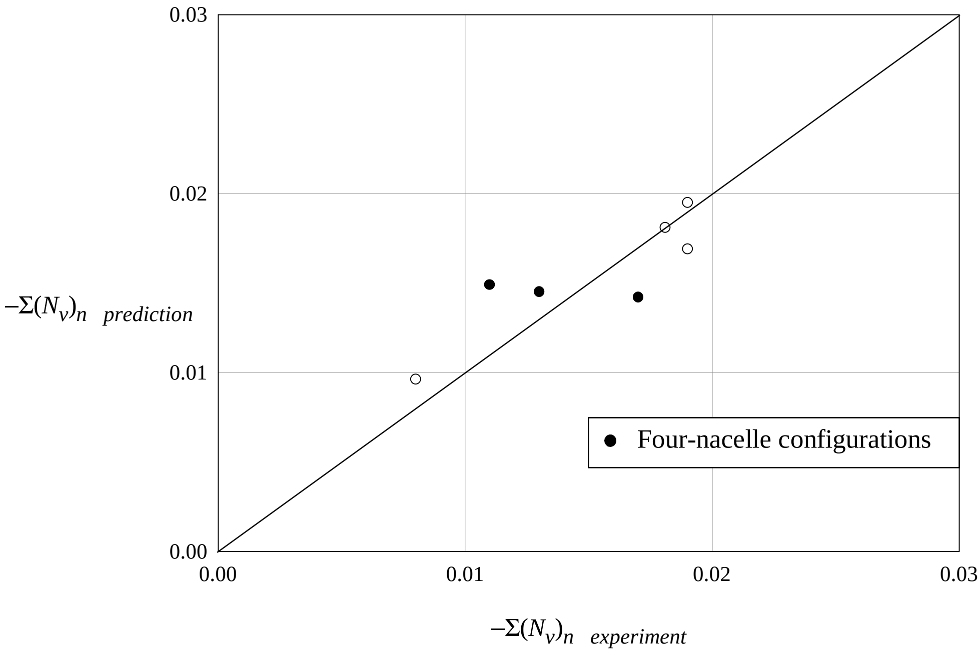

Sketch A4.2

Table A4.1 shows the ranges of geometric parameters covered by the experimental data.

TABLE A4.1

Parameter	*Range*
A	7.5 to 10
l_n/s	0.16 to 0.30
$l_n/w_{n\ max}$	1.6 to 2.7
m_0/s	0.2 to 0.4
s_n/s	0.29 to 0.52
$w_{n\ e}/s$	0.055 to 0.092
$w_{n\ max}/s$	0.092 to 0.13
$w_{n\ e}/w_{n\ max}$	0.58 to 0.73
z_n/s	0.056 to 0.13
$(z_n - 0.5w_{n\ max})/w_{n\ max}$	0.2 to 0.8
$(z_n + 0.5w_{n\ max})/w_{n\ max}$	1.2 to 1.8

A5. ADDITIONAL DERIVATION

A1. MORGAN, H.L. PAULSON, J.W. — Low-speed aerodynamic performance of a high-aspect-ratio supercritical-wing transport model equipped with full-span slat and part-span double-slotted flaps. NASA Tech. Paper 1580, 1979.

A6. EXAMPLE

Calculate the nacelle contribution to the derivatives Y_v and N_v for the configuration shown in Sketch A6.1. The wing reference area is $S = 194.3\ \text{m}^2$.

From Equation (A4.1)

$$
\begin{aligned}
(Y_v)_n &= -\pi w_{n\ max}^2 \left(\frac{z_n + 0.5 w_{n\ max}}{w_{n\ max}}\right)^{1.5} \Big/ S \\
&= -\pi 2.25^2 \left(\frac{1.38 + 0.5 \times 2.25}{2.25}\right)^{1.5} \Big/ 194.3 \\
&= -\pi 2.25^2 \times 1.175/194.3 \\
&= -18.69/194.3 \\
&= -0.0962
\end{aligned}
$$

and from Equation (A4.2)

$$
\begin{aligned}
(N_v)_n &= -\left[\pi w_{n\ max}^2 (m_0 - w_{n\ max}) + \pi w_{n\ e}^2 l_n\right] \Big/ Sb \\
&= -[\pi 2.25^2 (4.50 - 2.25) + \pi 1.35^2 \times 5.50] \Big/ (194.3 \times 38.4) \\
&= -[35.78 + 31.49]/(194.3 \times 38.4) \\
&= -0.00902\ .
\end{aligned}
$$

Thus the contribution of the nacelles to the lateral stability derivatives Y_v and N_v is $(Y_v)_n = -0.096$ and $(N_v)_n = -0.0090$.

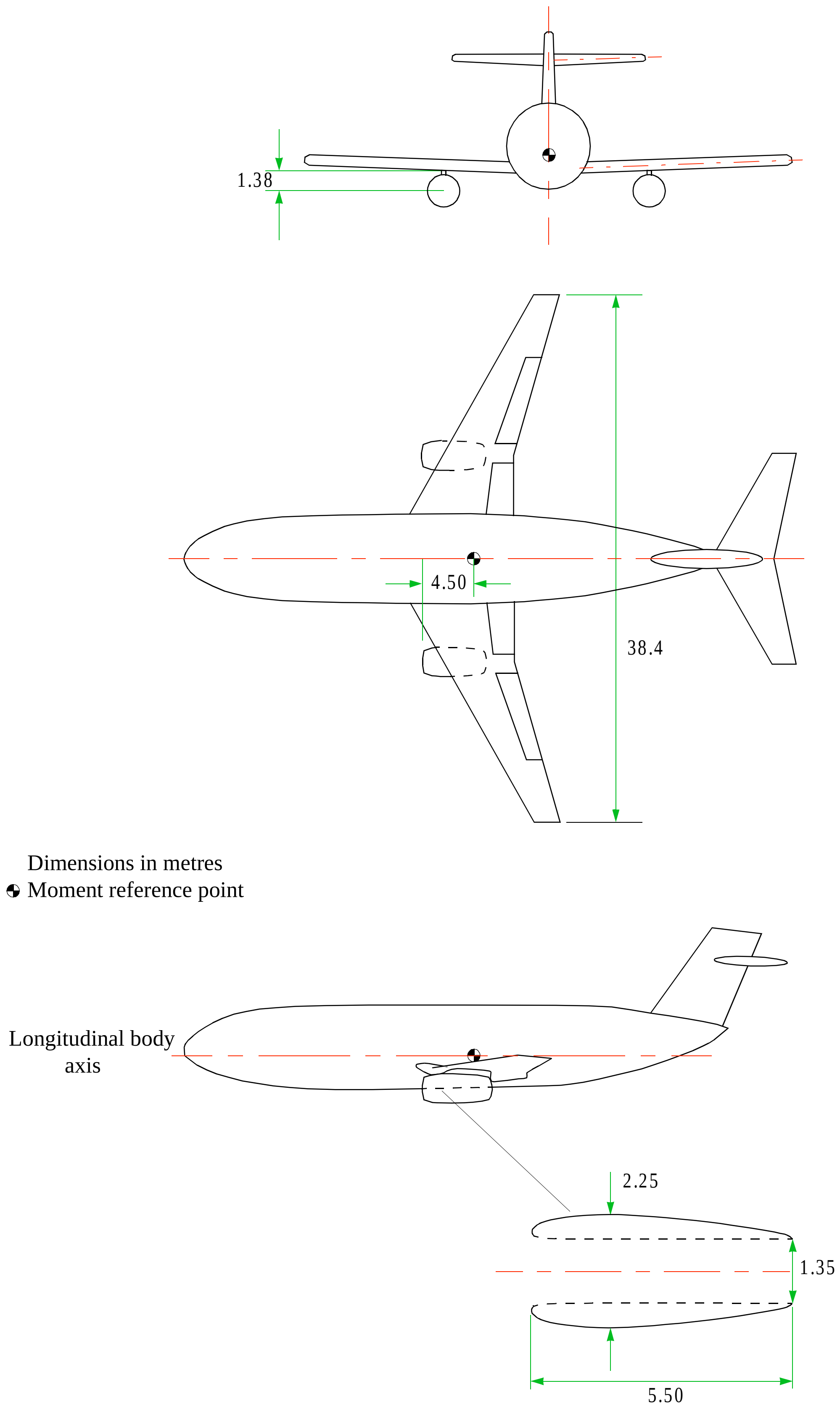

Sketch A6.1 Aircraft Geometry

THE PREPARATION OF THIS DATA ITEM

The work on this particular Item, which supersedes Item No. Aero A.07.01.01, was monitored and guided by the Aerodynamics Committee which first met in 1942 and now has the following membership:

Chairman
Mr P.K. Jones – British Aerospace, Manchester Division

Vice-Chairman
Mr J. Weir – Salford University

Members
Mr D. Bonenfant – Aérospatiale, Toulouse, France
Mr E.A. Boyd – Cranfield Institute of Technology
Mr K. Burgin – Southampton University
Mr E.C. Carter – Aircraft Research Association
Mr J.R.J. Dovey – British Aerospace, Warton Division
Mr H.C. Garner – Royal Aircraft Establishment
Mr A. Hipp – British Aerospace, Stevenage-Bristol Division
Dr B.L. Hunt – Bristol University
Mr J. Kloos* – Saab-Scania, Linköping, Sweden
Mr J.R.C. Pedersen – Independent
Mr I.H. Rettie* – Boeing Aerospace Company, Seattle, Wash., USA
Mr F.W. Stanhope – Rolls-Royce Ltd, Derby
Mr J.W.H. Thomas – British Aerospace, Hatfield-Chester Division
Mr H. Vogel – British Aerospace, Weybridge-Bristol Division.

* Corresponding Member

The member of staff who undertook the technical work involved in the initial assessment of the available information and the construction and subsequent development of the Item was

Mr R.W. Gilbey – Senior Engineer.